

Figure 1: Seasonal June-August (JJA) average of precipitation for 1990-1991: a) from Experiment B1 with weak re-evaporation, contours are drawn for 1.0, 2.0, 4.0, 8.0, and 16.0 mm d^{-1} ; b) as (a) except for Experiment B2 (moderate re-evaporation); c) as (a) except for Experiment B3 (strong re-evaporation); d) as (a) except for Xie-Arkin precipitation data.

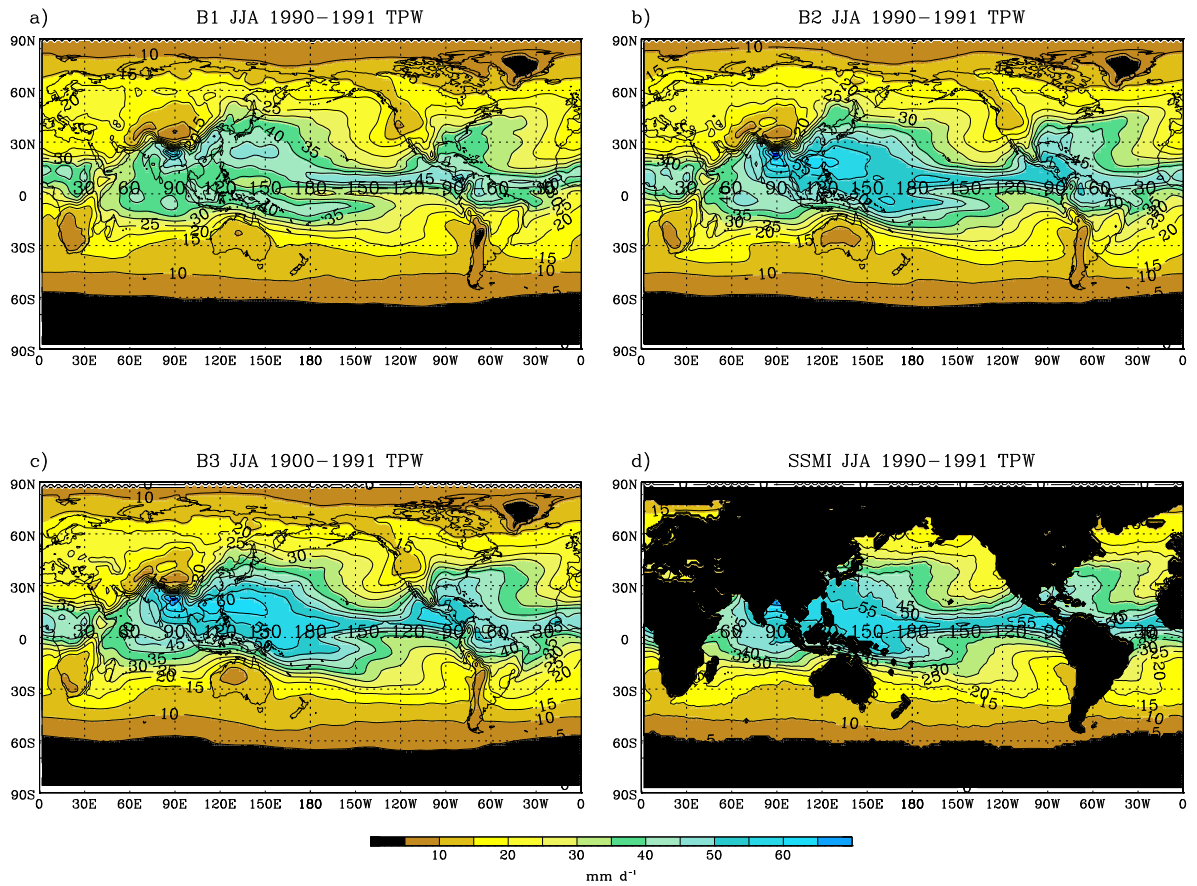


Figure 2: Total precipitable water for JJA 1990-1991 as a function of latitude and longitude: a) Experiment B1 (weak re-evaporation); b) Experiment B2 (moderate re-evaporation); c) Experiment B3 (strong re-evaporation); d) SSMI observational estimate. Contour interval is 5 kg m^{-2}

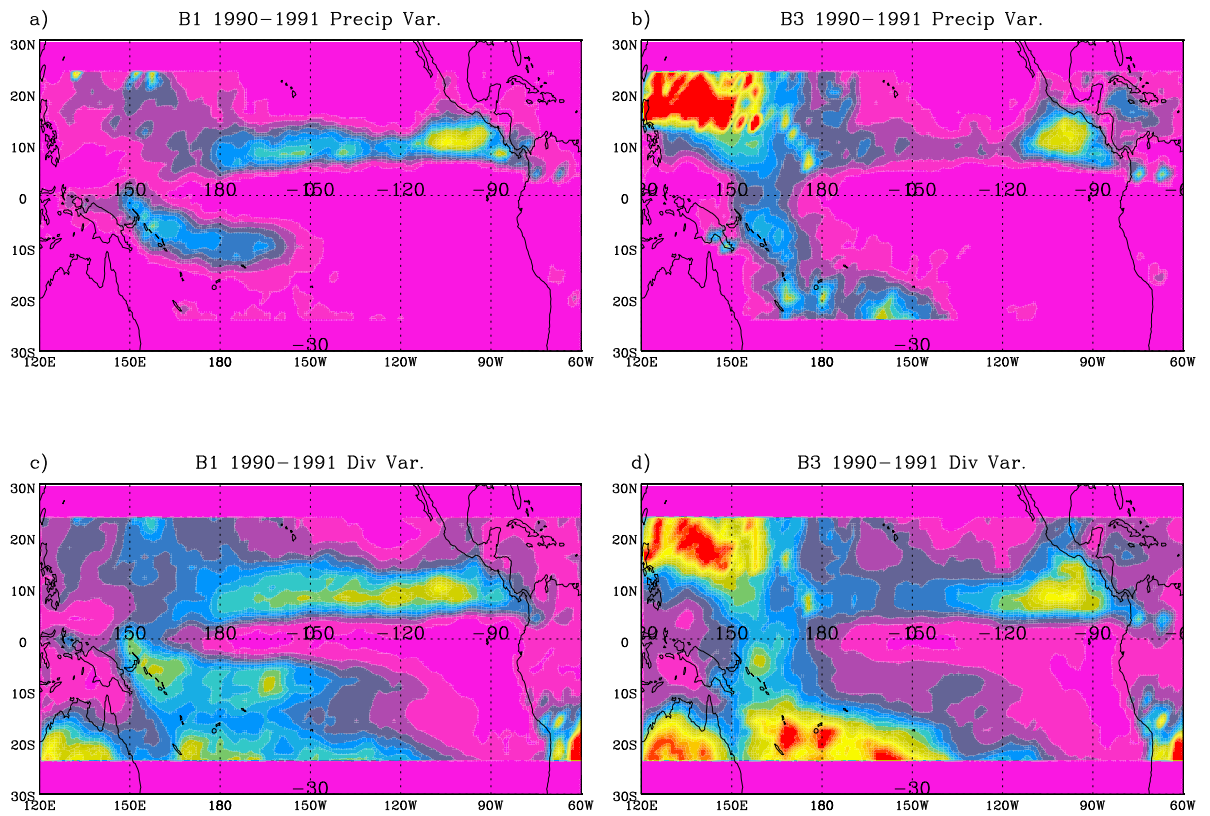


Figure 3: Mean precipitation and vertical motion variance from transient disturbances with time scales less than 31 d.

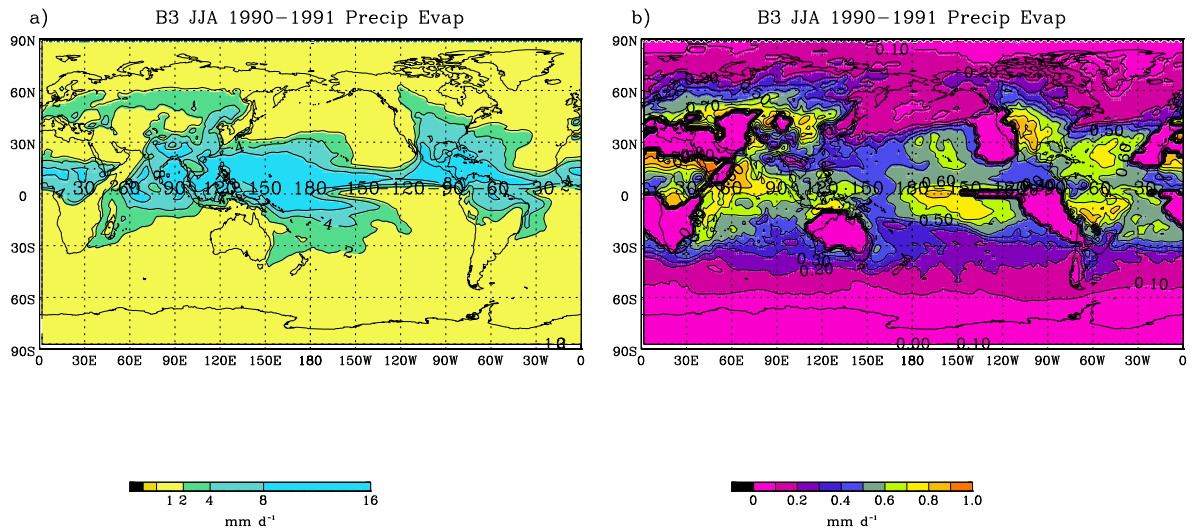


Figure 4: a) Mass-weighted, vertical integral of rain re-evaporation $\langle \mathcal{R} \rangle$ for JJA 1990-1991 in Experiment B3 (strong re-evaporation) as a function of latitude and longitude. Units are mm d^{-1} as for precipitation. Contour levels are 1.0, 2.0, 4.0, 8.0, and 16.0 mm d^{-1} as in Figures 1-4. b) Ratio of $\langle \mathcal{R} \rangle$ to total precipitation generated, i.e., $\langle \mathcal{R} \rangle + \mathcal{P}$ where \mathcal{P} is the precipitation flux at the surface. Values over 0.5 imply that over half of the rain water generated by the model evaporates before reaching the surface.

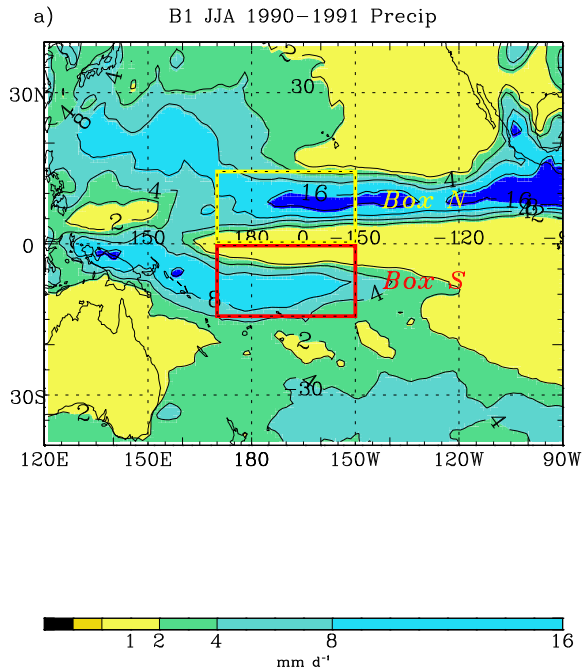


Figure 5: Domains used for profile and water budget analyses, shown over precipitation fields for JJA 1990-91 from Exp B1. The thick red line shows “Box S”, which is bounded by 170°E on the west, 150°W on the east, 14°S on the south and by the Equator on the north. It contains a significant portion of the spurious southern ITCZ that forms with weak re-evaporation. Box N is bounded by 170°E, 150°W in the zonal direction and by the Equator and 14°N in the meridional.

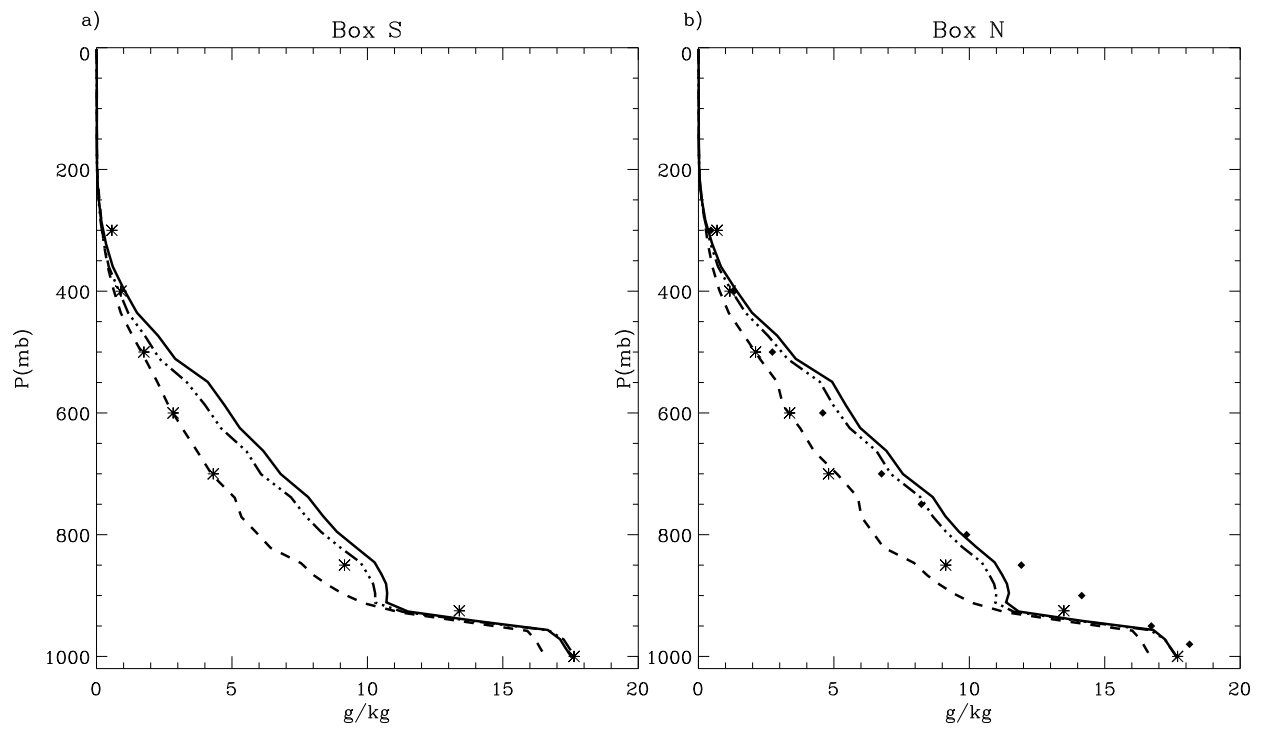


Figure 6: Box averaged profiles of specific humidity (left) and temperature (right) in Box S for JJA 1990. Thin solid lines show profiles for Exp B3, and dashed lines for Exp B1. The “*” symbol shows the NCEP re-analysis profiles for the same period.

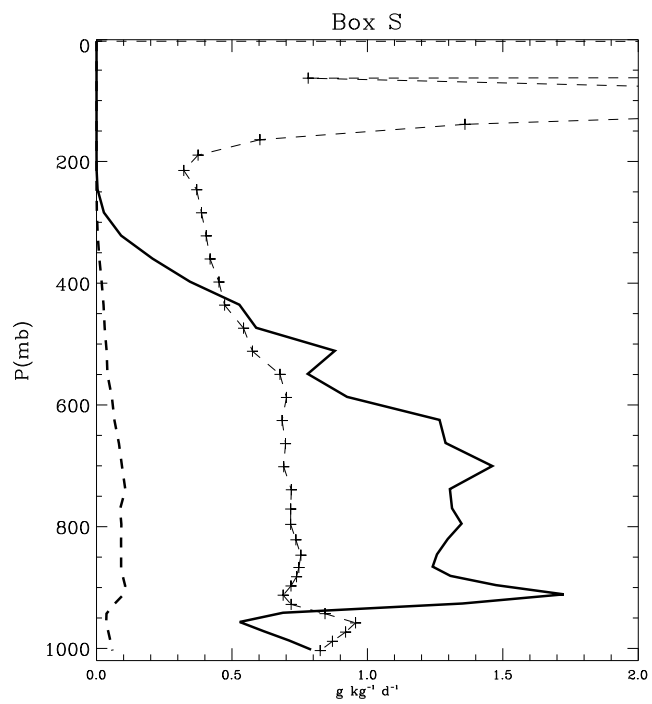


Figure 7: Box averaged profiles of \mathcal{R} moisture tendency due to re-evaporation of precipitation in Box for JJA 1990 in Exp B3 (thick solid line) and Exp B1 (thick dashed line). Units are $\text{g kg}^{-1} \text{d}^{-1}$. Crosses show corresponding relative humidity profile on a scale of 0-1 for Exp B3.

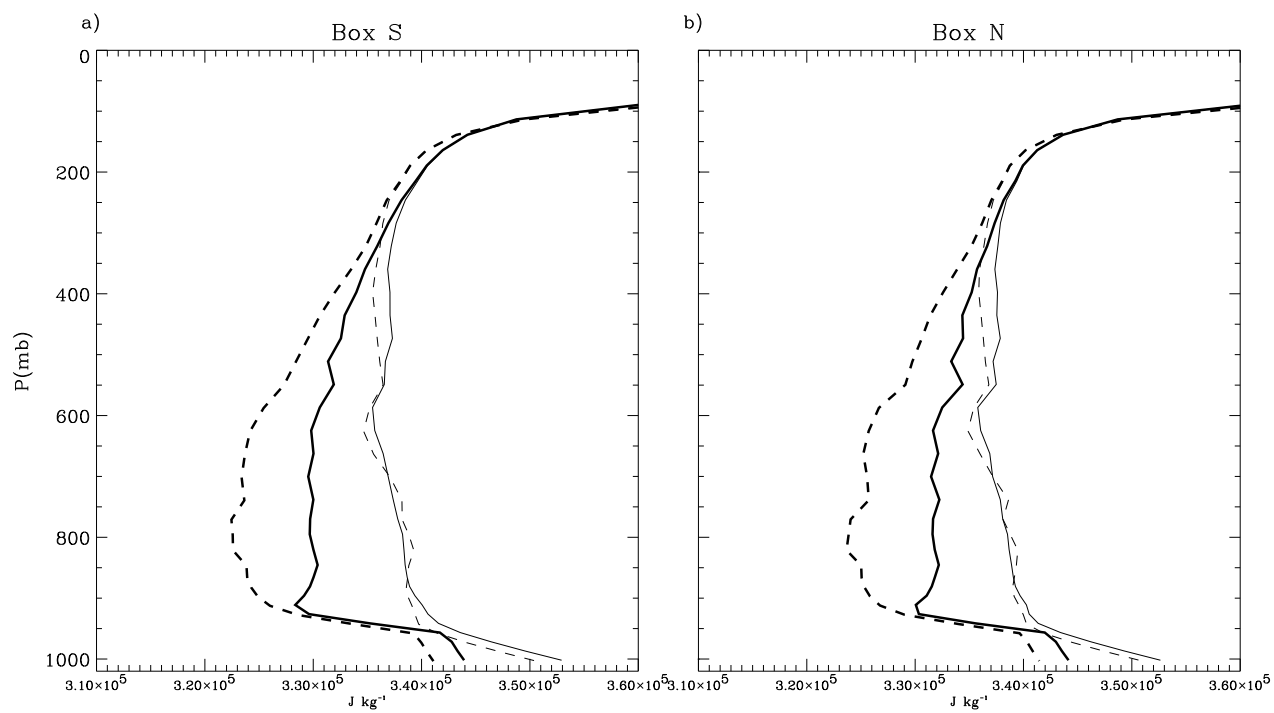


Figure 8: Box averaged profiles of moist static energy.

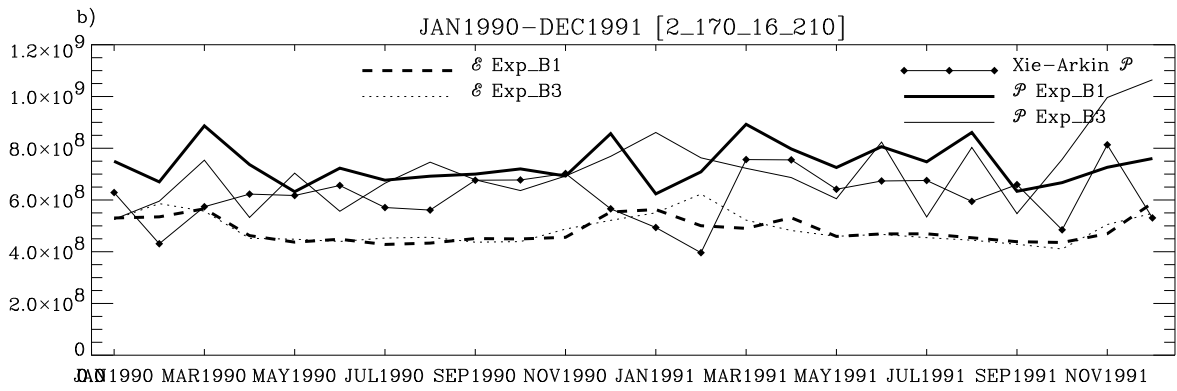
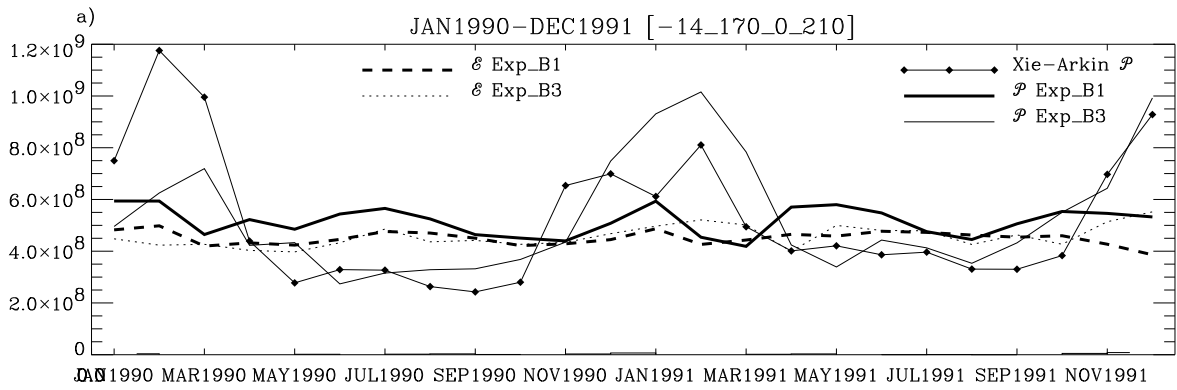


Figure 9: Box averaged water vapor budgets

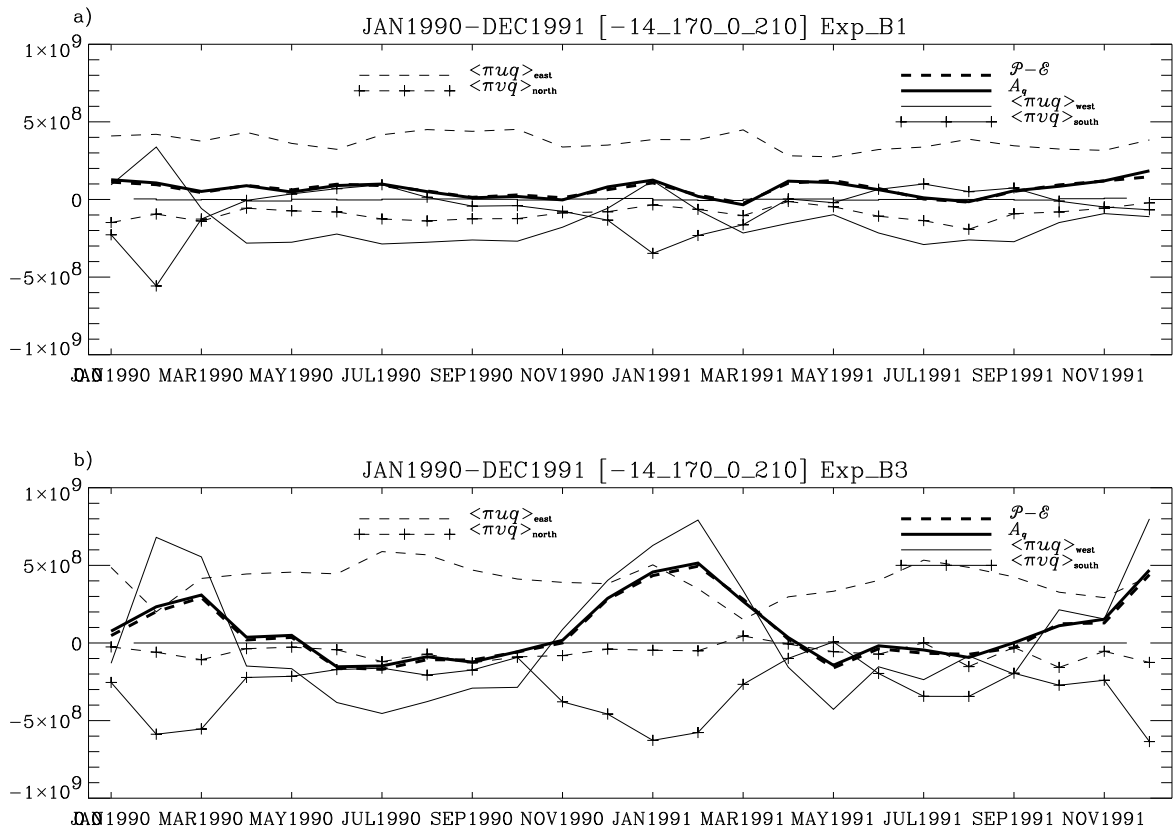


Figure 10: Box averaged water vapor budgets

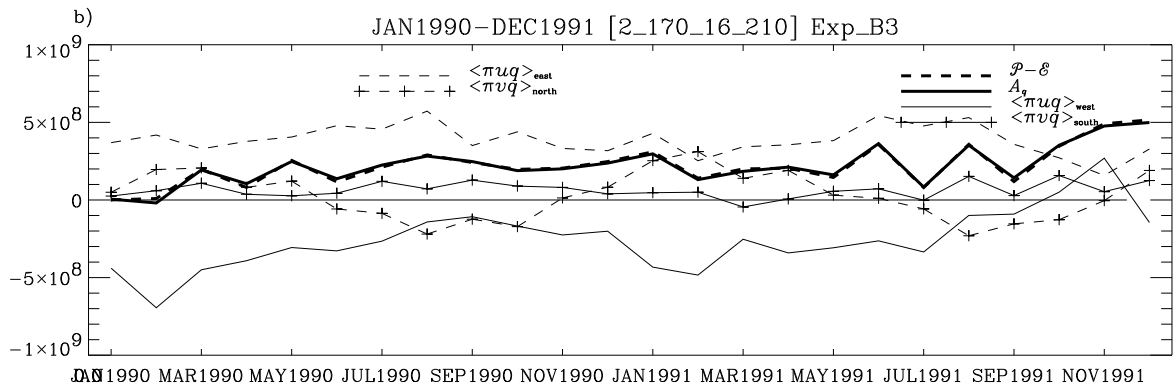
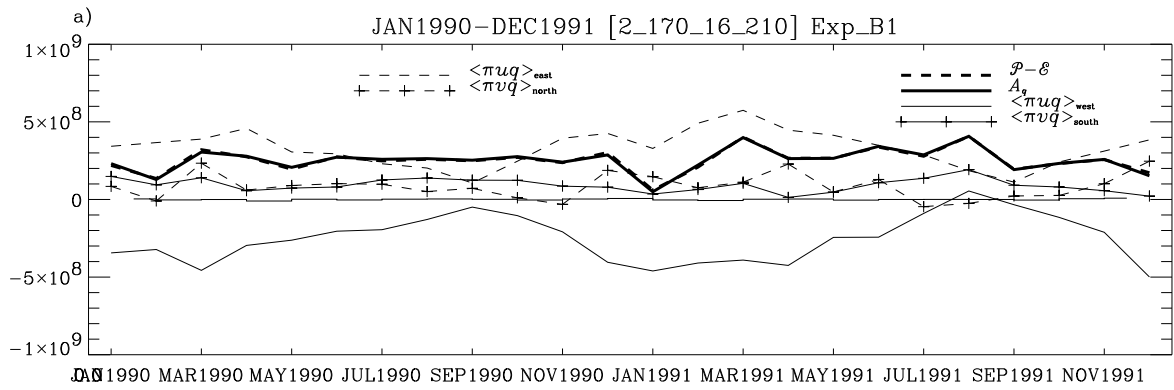


Figure 11: Box averaged water vapor budgets

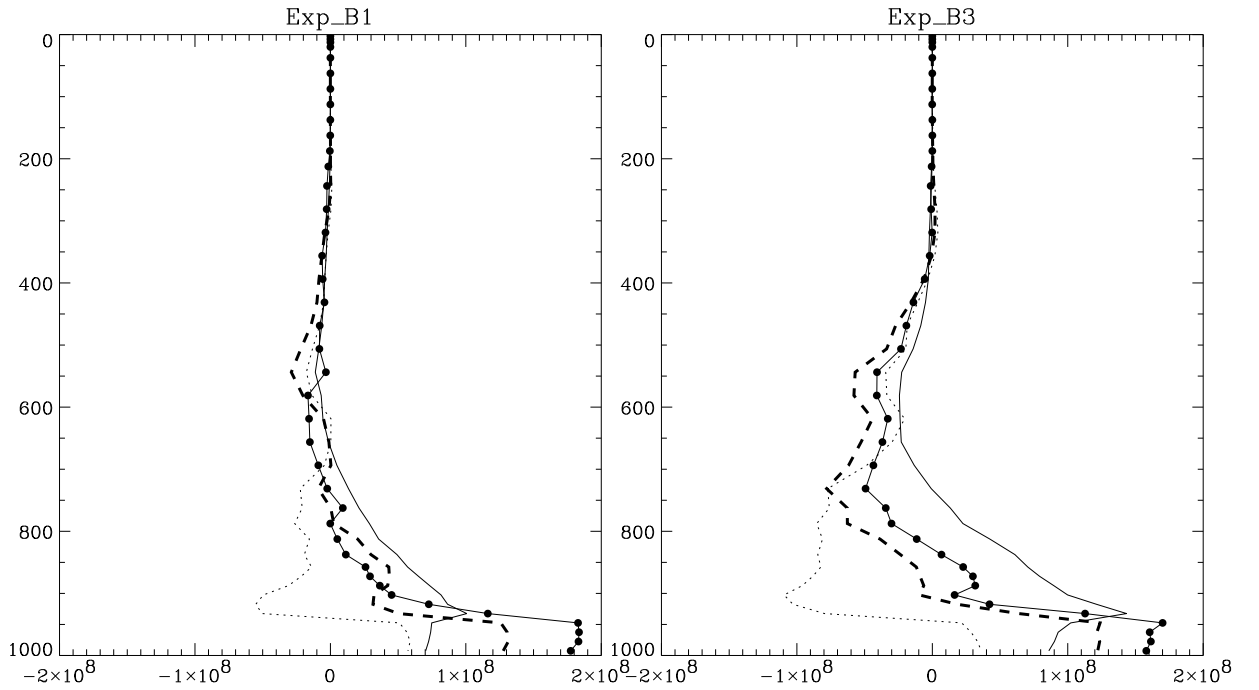


Figure 12: Box averaged profiles of water vapor flux quantities for JJA 1990 in Box S. Left panel shows results for Experiment B1 (weak re-evaporation), right panel for Experiment B3 (strong re-evaporation). Thin solid lines show $\langle \overline{\pi u q^\phi} \rangle_{\text{west}}^S - \langle \overline{\pi u q^\phi} \rangle_{\text{east}}^S$, thin dotted lines show $\langle \overline{\pi v q^\lambda} \rangle_{\text{south}}^S - \langle \overline{\pi v q^\lambda} \rangle_{\text{north}}^S$, and thick dashed lines show $\langle \overline{\pi u q^\phi} \rangle_{\text{west}}^S - \langle \overline{\pi u q^\phi} \rangle_{\text{east}}^S + \langle \overline{\pi v q^\lambda} \rangle_{\text{south}}^S - \langle \overline{\pi v q^\lambda} \rangle_{\text{north}}^S$, i.e., the net advective water vapor transport into Box S. The solid circles show the area integral of $q \vec{\nabla} \cdot (\pi \vec{V}_h)$, the component of the net transport into Box S accomplished by convergent winds.